Published in AJSE, Vol:21, Issue: 1
Received on 8th December 2021
Revised on 11th June 2022
Accepted on 12th June 2022

AIUB JOURNAL OF SCIENCE AND ENGINEERING
ISSN: 1608 – 3679 (print) 2520 – 4890 (Online)

Highly Directive Graphene Based Hybrid Plasmonic Nanoantenna for Terahertz Applications

Richard Victor Biswas and Farhadur Arifin

***Abstract*— To satisfy the necessity for elevated data transmission rates in 5G and beyond networks, terahertz band communication (0.1 - 10 THz) is envisaged as a crucial wireless technology. Two-dimensional graphene nanomaterial is being extensively integrated into the plasmonic antennas as it allows them to resonate in the terahertz wave spectrum. A graphene-based hybrid terahertz plasmonic nano-scale antenna has been modeled to acquire a maximum gain and directivity of 8.1 dB and 8.23 dBi, respectively, by varying the conductivity of graphene via gate bias voltage. Moreover, a combination of several tailored radiating layers of silver, SiO_2 and graphene sheets is arranged in the proposed nanoantenna in such a way that the return loss (S_{11}) of -26.595 dB and wider bandwidth of 1241.3 GHz are obtained. It is evident that the proposed graphene-based hybrid plasmonic nanoantenna could be considered an ideal candidate for terahertz communication owing to its excellent radiation characteristics.**

***Index Terms*— Dielectric grating, Graphene plasmonic, Surface plasmon polariton, THz frequency spectrum**

I. Introduction

Due to the ever-increasing number of next-generation wirelessly connected devices requiring a data transmission rate of 10-100 Gbps [1], wireless communications in the terahertz (THz) band are becoming crucial which inevitably fulfills this speed demand. The low THz frequency spectrum (from 0.1 to 10 THz) lies in between the microwave and the mid-infrared bands. THz wave does not harm to the human body and change the chemical structures because of its low photon energy (e.g., 4 meV at 1 THz), low scattering, and non-ionizing radiation. These waves can penetrate through materials, paper, cardboard, textiles, plastics, wood, ceramics, semiconductors and so on which are impervious to other parts of the electromagnetic spectrum. Although the THz band has several benefits, one of the shortcomings of this type of radiation is high path loss because of atmospheric molecular absorption. This hinders its application to some extent [2-6]. To further increase the communication distance between THz transmitter and receiver, generated radiation power should be effectively transmitted through directional antennas.

Antennas in nanometer scale (nanoantenna) radiate in THz band efficiently having wider bandwidth (BW) and considerably high spatial resolution of around 1 mm. Therefore, numerous fields of application namely terabit-per-second (Tbps) secure wireless communication links [7], biology and medicine [8, 9], rotational, vibrational, and transitional characterization of materials [10], agriculture [11], security and inspection [12] and astronomy [13] are extensively incorporating these nanoantennas. Over the last couple of years, many researchers have successfully realized high-performance photo-conductive antennas [14], modulators, quantum cascade lasers working as feeding sources [15], optical down-conversion systems, detectors operating at THz regime. Compact directional wide-band horn antenna [16], lens antenna [17] and other innovative antennas with gains around 55dB [18-20] are already in use.

On the other hand, Yagi-Uda antenna [21], MEMS antenna [22], Fractal antenna [23], leaky wave antenna [24], log-periodic antenna [25] and bow-tie antenna [26] have been studied for low THz band applications (e.g., wireless communication nanolink). A few limitations of these nanoantennas are as follows: relatively large antenna size (e.g., 5500 × 5592 um^2 [21], 90 × 80 um^2 [22], and so on) and high frequency feeding source required to excite (e.g., continuous wave (CW) THz source [21], substrate integrated waveguide [24] and etc.).

To attain the transmission BW as high as 100 GHz, graphene-based THz plasmonic antenna could be one of the promising alternatives [27, 28]. Graphene is an allotrope of carbon, whose atoms are arranged in a two-dimensional hexagonal lattice structure. It has amazing optical and mechanical properties, and electrical conductivity which allows the propagation of high-frequency electrical signals. It possesses a mean free path of 300-500 nm for ballistic carrier transport and the carrier mobility in the range of 8000 - 10000 $cm^2V^{-1}s^{-1}$. Because of this extraordinarily high carrier mobility at THz frequencies, graphene boosts the propagation of confined electromagnetic Surface Plasmon Polariton (SPP) waves [29, 30]. At the edge of a conductor and dielectric, the confined SPP waves are produced. The exploration of new graphene-based THz plasmonic nanoscale antennas is inevitable due to the intrinsic tunability of graphene conductivity by electrostatic biasing and the highly restricted wavelength of SPP waves. For modulation & demodulation [31-36], signal generation & detection [37-39] and nanoscale sensing [40] in THz regime, these type of reconfigurable nanoantennas are frequently considered.

Most of the graphene-based THz antennas in the existing literatures [41-49] have some downsides: limited BW, gain and directivity. In [45], a graphene based miniaturized THz patch antenna operating in 5.39-5.61 THz resonant frequency range is proposed with a low BW of 218 GHz and a limited gain of 3.9 dB, still it has a relatively high directivity of 5.429 dBi. As reported in [50], a gain of 5.986 dB and a peak directivity of 6.5 dBi are achieved from an ultrawide-band (UWB) circular graphene patch antenna; however, a maximum BW of 504 GHz is stated. A graphene plasmonic antenna operating around 0.81 THz with a minimum peak -directivity of 4.5 dBi is proposed in [51]. In [52], another graphene plasmonic nanoantenna with

a maximum BW of 2420 GHz (2.56 THz - 4.98 THz) is proposed which offers a moderate directivity of about 5.56 dBi.

In this paper, a graphene-based hybrid plasmonic nanoantenna (GHPNA) has been proposed and analyzed for low THz band applications (0.1 - 10 THz). The modified layers of silver (Ag), graphene sheet with cylindrical air defects, and SiO_2 grating forming an uneven waveguide-like structure have been chosen to design our proposed nanoantenna. Furthermore, the metamaterial-based subwavelength slots - on top of SiO_2, Ag, and graphene perturbed layers - ensure excellent radiation characteristics.

The subsequent sections of this paper have been arranged as follows. The properties of graphene in terms of surface plasmon polariton, plasmonic resonance, dispersion relation, conductivity, surface impedance, and power absorption have been presented in section II. In section III, the process of modeling the proposed hybrid nano-scale antenna has been covered. In the "Simulation and Results" section, the outcomes of our nanoantenna have been discussed and the comparison among reported graphene-based antennas with our proposed one has been incorporated. Lastly, conclusions of this research work have been drawn in "Conclusion".

II. Properties of Graphene

A. Surface Plasmon Polariton, Plasmonic Resonance & Dispersion Relation of Graphene

In free space, the dispersion relation of the supported transverse magnetic (TM) plasmons or the SPP wave vector (k_{SPP}) of graphene sheet can be represented as [53-55]

$$k_{SPP} = k_0\sqrt{1-(\frac{2}{\eta_{eff}\sigma_g})^2} \approx \frac{\hbar\omega^2}{2\alpha\mu_c c} \quad (1)$$

$$\eta_{eff} = \sqrt{1-\frac{4\mu_0}{\varepsilon_0\,(\sigma_g)^2}} = \frac{\lambda}{\lambda_{SPP}} \quad (2)$$

where the complex conductivity (σ_g) of graphene is a function of chemical potential (μ_c) and angular frequency is ω. k_0 and η_{eff} are the free-space wavenumber and effective intrinsic impedance of graphene sheet, respectively. The mode index or effective intrinsic impedance of graphene is related to both the free-space permeability (μ_0) and the absolute permittivity (ε_0) of graphene [56]. By changing the bias voltage across the graphene nodes, which in turn varies the chemical potential of it, the SPP wave vector of graphene sheet can be calculated. Again, it is obvious from the dispersion relationship of TM plasmons that k_{SPP} varies as a second order function of the resonant frequency (f_r) while the reduced plank's constant (ħ), the fine structure constant ($\alpha = \frac{e^2}{\hbar c}\frac{1}{4\pi\varepsilon_0} = \frac{1}{137}$) [57], the charge of electrons (e) and the velocity of light in vacuum (c) remain unchanged.

$$\mathrm{L_g} = \mathrm{m}\frac{\lambda}{2\eta_{\mathrm{eff}}} = \mathrm{m}\frac{\lambda_{\mathrm{SPP}}}{2} = \mathrm{m}\,\frac{\pi}{\mathrm{k_{SPP}}} \quad (3)$$

Using Eq. (3), the length of the graphene layers (L_g) can be estimated considering the plasmonic resonances of SPP waves [58] where m is the resonant mode number, λ is the wavelength of the incident radiation through the discrete port, and λ_{SPP} is the wavelength of SPP waves.

$$L_g = m\,\frac{2\pi\alpha\mu_c c}{\hbar\omega^2} \quad (4)$$

$$f_r = \sqrt{m\frac{\alpha\mu_c c}{2\pi L_g \hbar}} \quad (5)$$

Manipulating the SPP wave vector in Eq. (1) & (3) leads to the expression of L_g in Eq. (4), which is inversely proportional to the resonant frequency (f_r) exhibited in Eq. (5). Thus, the length of the graphene layers is increased for a lower application specific resonant frequency.

B. Conductivity, Surface Impedance, Power Absorption of Graphene

$\sigma_g\ (\omega,\mu_c,\Gamma,T)$ is an amalgamation of both inter-band and intra-band transitions as expressed in Eqs. (6), (7) & (8), which is in compliance with the Kubo formula [59]. K_B and T are the Boltzmann constant and temperature at 300K, correspondingly.

$$\sigma_g = \sigma_{intra} + \sigma_{inter} \quad (6)$$

$$\sigma_{intra}(\omega,\mu_c,\Gamma,T) = -j\,\frac{e^2K_BT}{\pi\hbar^2(\omega-j\Gamma)}\,\{\frac{\mu_c}{K_BT} + 2\ln\,(e^{-\frac{\mu_c}{K_BT}}+1)\} \quad (7)$$

$$\sigma_{inter}(\omega,\mu_c,\Gamma,T) = \frac{-je^2}{4\pi\hbar^2}\,\ln\,(\frac{2|\mu_c|-(\omega-j\Gamma)\hbar}{2|\mu_c|+(\omega-j\Gamma)\hbar}) \quad (8)$$

The characteristic impedance of the supported transverse magnetic (TM) plasmons in the graphene sheet is determined as follows [53-55]:

$$Z_g = Z_C = \frac{1}{\sigma_g} = R_g + jX_g = \frac{k_{SPP}}{\omega\varepsilon_0\varepsilon_{r(eff)}} \quad (9)$$

where R_g and X_g are the surface resistance and reactance of the graphene sheet, respectively; $\varepsilon_{r(eff)}$ is the effective dielectric constant of the surrounding media. The chemical potential (μ_c) and the electrostatic biasing gate voltage (V_g) are strongly intertwined to each other [60]:

$$\mu_c = E_f = \hbar v_f\sqrt{\frac{\pi\varepsilon_{ox}\varepsilon_0 V_g}{et_{ox}}} = \hbar v_f\sqrt{\frac{\pi C_{ox}V_g}{e}} \approx \hbar v_f\sqrt{\pi N} \quad (10)$$

where v_f is the velocity of electrons in Fermi energy level ($\approx 10^6$ ms^{-1}), ε_{ox} is the permittivity of SiO_2 layer, t_{ox} is the oxide thickness, C_{ox} ($=\frac{\varepsilon_{ox}\varepsilon_0}{t_{ox}}$) is the electrostatic gate capacitance/area, and N ($\approx \frac{C_{ox}V_g}{e}$) is the carrier concentration [61]. Hence, more biasing voltage establishes more chemical potential of graphene. As graphene regains a uniform charge density upon applying a biasing voltage, the relaxation time (τ) is improved to at least 0.1 ps and τ is given by [62]

$$\tau \approx \mu_c \hbar \sqrt{\frac{\pi N}{e v_f}} \quad (11)$$

C. Graphene Modeling

The epsilon-near-zero effect of graphene becomes prominent once the electrostatic gate bias voltage is applied [64, 65], resulting in a noticeable absorbed power of graphene given by Eqs. (12) & (13).

$$\varepsilon_g(\omega, \mu, \Gamma, T, \Delta) = 1 + \frac{j\sigma_g}{\omega \varepsilon_0 \Delta} \quad (12)$$

$$P_g = \frac{\mathrm{Re}(\sigma_g) E^2}{2} \quad (13)$$

In order to reconfigure our graphene-based plasmonic device with the dielectric function (ε_g) having a thickness of Δ = 0.34 nm [63], the chemical potential (μ_c) of 0.5 eV and the charge particle scattering rate (Γ) of 0.00051423 eV have been selected. Our hybrid graphene nano structure is able to absorb a wide range of powers (P_g) by adjusting the conductivity of graphene layer and the incident laser photon energy (E), which is indicated by Eq. (13) [64].

The connection among chemical potential, frequency and conductivity of graphene material has been extracted analytically with the help of Ansys Lumerical software, which uses the finite-difference time-domain method (FDTD). In Fig. 1, a direct correlation of the real and imaginary parts of σ_g with respect to μ_c has been illustrated.

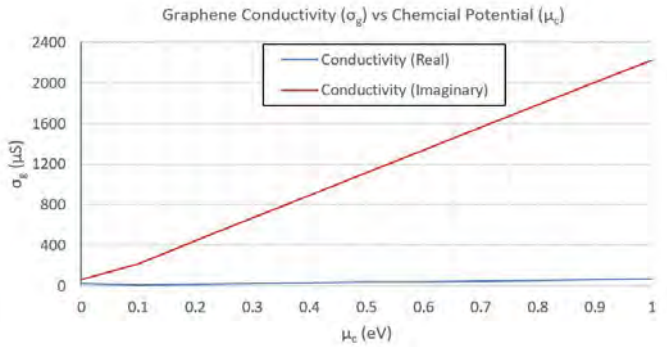

Fig. 1. Change in real and imaginary parts of conductivity curves of graphene with respect to chemical potentials (μ_c) ranges from 0 eV to 1 eV for τ = 0.1 ps at f_r =8.4 THz and T = 300 K

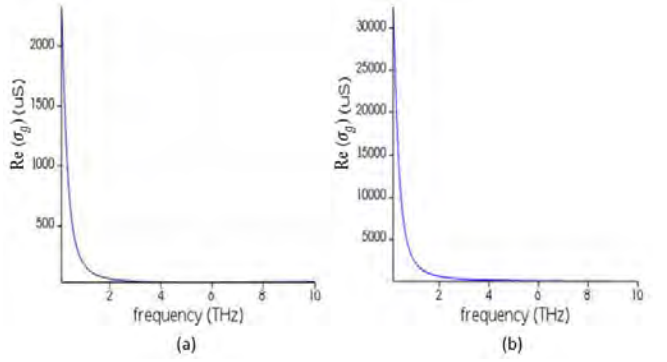

Fig. 2. Change in real, Re (σ_g), parts of conductivity curves of graphene as functions of frequency (1 THz – 10 THz) for (a) μ_c = 0.0 eV and (b) μ_c = 0.5 eV at T = 300 K

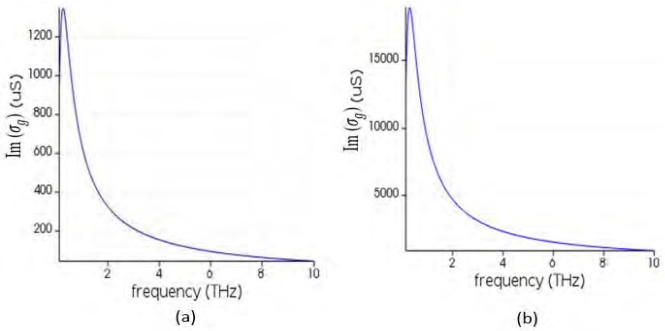

Fig. 3. Change in imaginary, Im (σ_g), parts of conductivity curves of graphene as functions of frequency (1 THz – 10 THz) for (a) μ_c = 0.0 eV and (b) μ_c = 0.5 eV at T = 300 K

The graphical representations of conductivity of graphene with respect to the THz frequency depicted in Fig. 2 and 3 are similar to the ones reported by Llatser, et.al [79]. At μ_c = 0.5 eV, negative correlations of the real as well as imaginary parts of conductivity with reference to frequency (0.1 - 10 THz) are apparent as shown in Fig. 2 and 3. The real parts of graphene conductivity, Re (σ_g), nearly equal to zero at f_r = 8.4 THz for μ_c = 0 eV and 0.5eV, however Im (σ_g) > 50 μS and Im (σ_g) > 150 μS for the respective chemical potentials. When $\mu_c < \frac{\hbar\omega}{2}$, the maximum power absorption of graphene can be found where the imaginary part of the inter-band contribution dominates. Thus, for μ_c = 0 eV with no bias voltage, graphene acts as a transparent medium. Conversely, graphene behaves as an absorptive medium at 8.4THz for μ_c = 0.5 eV.

III. Design of the Proposed Graphene-based Nanoantenna Structures

As demonstrated in Fig. 4, each layer of the proposed GHPNA is modeled in the finite element method (FEM) simulator called "CST Microwave Studio". The ground plane of GHPNA is silver (Ag) and this nanoantenna is covered by a perturbed graphene structure (in the 2nd last stage). Ag has been preferred rather than gold layer because of the better surface plasmon polaritons (SPPs) excitation of silver at low-terahertz and optical regime. Moreover, Ag offers smaller charge particle scattering rate (Γ) of 0.02eV, lower loss and lower fabrication cost, making it an ideal choice for our hybrid graphene nanoantenna [67, 68]. Therefore, Ag ground plane has been modeled as shown in Fig. 4 (a). A graphene sheet with air defects has been placed on top of the ground plane depicted in Fig. 4 (b). To mitigate the surface wave excitation loss in the thick dielectric grating (SiO_2) with high permittivity, periodic hollow air defects in the graphene sheet with 200 nm thickness have been into account. Besides, the shock waves at the dielectric-graphene-silver interfaces in the low THz range have been minimized by selecting that porous graphene sheet [69, 70]. The graphene sheet with air defects also suppresses the surface wave propagation, improving directivity, gain, BW, and other performance parameters of the antenna. The reduction of cross polarization and back-end fire radiation can also be detected from such structure [71, 72].

Referring to Fig. 4 (c), the grating of SiO_2 has been introduced in order to convert the SPPs into leaky waves with its irregular waveguide-like structure. For beamforming THz nanoantenna applications, dielectric gratings with periodic shapes are being extensively applied [73-76]. A group of four intermediate rectangular graphene patches has been incorporated to control the main lobe direction of radiation pattern and intensity of the nanoantenna as illustrated in Fig. 4 (d). Every patch can be regulated by applying different gate biases, which varies the absorption power of the overall antenna structure.

As depicted in Fig. 4 (e-g), eight directors composed of SiO_2, Ag, and graphene materials have been designed to obtain a unidirectional radiation pattern along z-axis. Again, referring to the same figures, four rectangular sets of metamaterial-based subwavelength slots of variable lengths in four corners of the graphene patches have been formed as connecting nodes of one feedline and two directors. For inducing the electric and magnetic dipole moments [77] and ensuring a wider impedance BW [78], this periodic array of metamaterial slots has been added to the proposed nanoantenna.

A discrete port with internal impedance of 50Ω has been chosen for our proposed nano-scale antenna to stimulate as shown in Fig. 4 (h), which is an alternative of either a Femto second laser or a quantum dot source [49]. To manage the radiation of the discrete port, each intermediate graphene patch has been separated by 100 nm from each one of them. The starting and ending points of the discrete port have been defined by choosing any two feed points (considered 1st and 4th feed points) of the top Ag layer. As depicted in Fig. 4(h), a red cone sitting in the center of the line and a blue line connecting two points indicate a discrete port source and a perfectly conducting electrical wire, respectively.

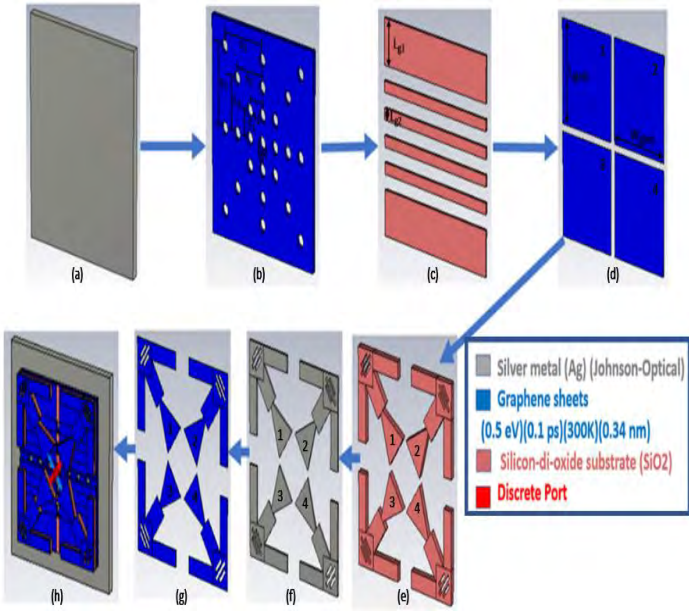

Fig. 4. Customized layers of various materials (Ag, Graphene & SiO_2) to observe the antenna resonance at 8.4THz. Discrete port is an illumination port, resembling Femto second laser or quantum dot source

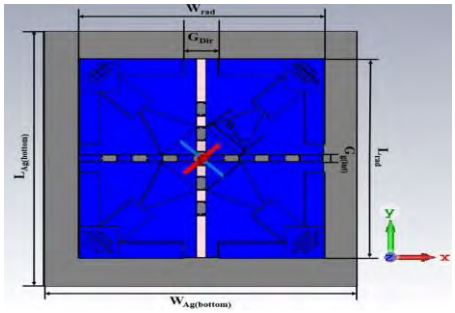

Fig. 5 (a). Top schematic view of the optimized GHPNA

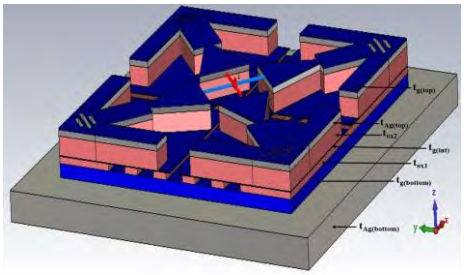

Fig. 5 (b). Side schematic view of the optimized GHPNA

In order to tune the nanoantenna at 8.4 THz, parametric analysis has been conducted in CST Microwave Studio. In Table I and Fig. 5 (a, b), the optimized dimensions of several layers of the proposed nanoantenna have been given. Referring to Eq. 14, the total length (L) and width (W) of the radiating structure in the nanoantenna are chosen dynamically depending upon the operating frequency (f_r) [66]:

$$L, W \propto \frac{1}{f_r} \tag{14}$$

For our nanoantenna, each one of the overall length and width of the radiating segment has been optimized to be 2800 nm and thickness of it to be 315nm for low THz applications (0.1-10 THz), e.g., wireless communication nanolinks.

TABLE I. OPTIMIZED DIMENSIONS OF THE PROPOSED GHPNA

Structure Dimension		Values (nm)
Cylindrical Air Gap Periodicities in the Bottom Graphene	S_1	350
	S_2	700
	S_3	1050
Air Gap Diameter in the Bottom Graphene	a	180
Bottom Graphene Thickness	$t_{Ag(bottom)}$	200
Dielectric Grating Lengths	L_{g1}	600
	L_{g2}	150
Dielectric Thicknesses	t_{ox1}	45
	t_{ox2}	125
Intermediate Graphene Length and Width	$L_{g(int)}$	1350
	$W_{g(int)}$	1350
Intermediate Graphene Thickness	$t_{g(int)}$	5
Intermediate Graphene Gap	$G_{g(int)}$	100
Top Perturbed Graphene Layer Thickness	$t_{g(top)}$	10
Ag Ground Plane Length & Width	$L_{Ag(bottom)}$	3600
	$W_{Ag(bottom)}$	3600
Ag Ground Plane Thickness	$t_{Ag(bottom)}$	200
Midway Ag Layer Thickness	$t_{Ag(top)}$	40
Radiating Structure (Graphene, SiO_2, & Ag) Length and Width	L_{rad}	2800
	W_{rad}	2800
Director Gap	G_{Dir}	400
Feed Width	W_{feed}	565.69

IV. Simulation and Results

Our proposed nanoantenna has been designed and simulated successfully with the help of CST Microwave Studio. CST employs finite integration technique (FIT) in order to perform the transient analysis. Hexahedral-type mesh with default automatic mesh adaptation is processed to refine the design in CST during transient analysis.

Initially, a homogenous rectangular graphene patch and plain SiO_2 layer have been selected in place of the optimized graphene sheet with air defects and dielectric grating, respectively. Intermediate rectangular graphene patches and top radiating structure have been kept. Since return loss (-20.181 dB), gain (7.35 dB) and directivity (7.61 dBi) of such composite structure at 8.2 THz are not notable as compared to those of our proposed nano-scale antenna (Table II & III), the modified layers of graphene and SiO_2 have been taken into account. In another case, only intermediate rectangular graphene patches and top radiating structure have been placed above Ag ground plane, leading to S_{11} of -21.904 dB and BW of 1053 GHz at 7.4 THz. Again, the results are not up to the mark in contrast to ones we have for our proposed nanoantenna. Lastly, instead of both homogenous rectangular graphene patch and plain SiO_2 layer, only dielectric layer has been positioned between intermediate rectangular graphene patches and Ag ground plane. For low THz applications (0.1 – 10THz), such structure is not appropriate as it resonates at 29.4 THz, referring to Table II. Fig. 6 illustrates the S_{11} parameters for these initial arrangements of layer(s) in our proposed GHPNA. In order to further improve the radiation characteristics of our nanoantenna, holistic optimization process (geometry & dimension) has been conducted (Fig. 5 and Table I).

TABLE II. Radiation characteristics of our proposed nanoantenna possessing some initial structures

Primary Structures	Operating Frequency (f_r) (THz)	S_{11} (dB)	BW (GHz)
Rectangular Homogenous Graphene Sheet	8.2	-20.181	1427
Plain Dielectric			
Intermediate Graphene Patches Only	7.4	-21.904	1053
Only Plain Dielectric	29.4	-23.652	761

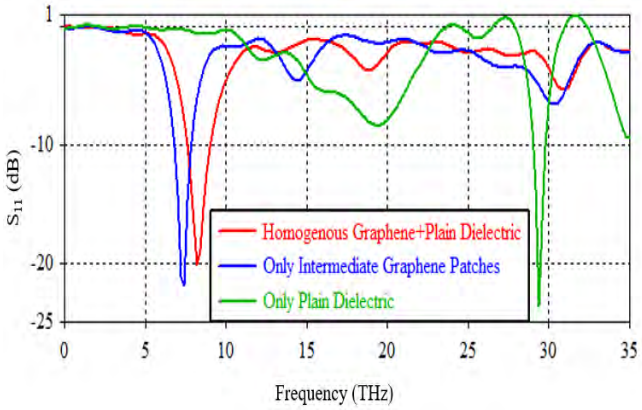

Fig. 6. Return losses (S_{11}) for different arrangements

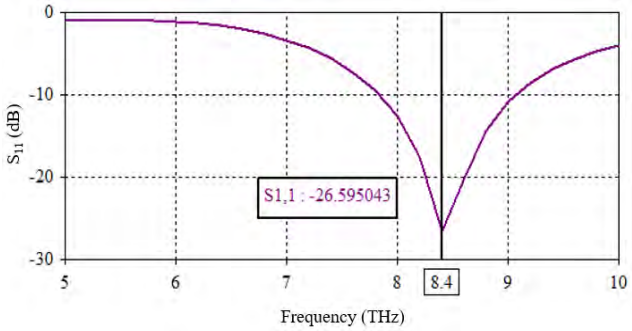

Fig. 7. Return Loss (S_{11}) of the proposed plasmonic antenna at 8.4THz

For a frequency of interest, low return loss (S_{11} < - 10 dB) specifies the parts of nanoantenna are well matched. Fig. 7. depicts the return loss and -10 dB impedance BW of -26.595 dB and 1.2413 THz, respectively, for our proposed plasmonic nanoantenna operating at 8.4 THz resonant frequency. In Fig. 8 (a) and Fig. 8 (b), the electric field and magnetic field patterns are shown, respectively. From Fig. 8 (a), an intense E-field for a phase of 90° is observed not only at the directors connected with the 1st and 4th feedlines but also at the graphene patches. Conversely, the E-field in the Ag ground plane fades away. A high H-field for a phase of 180° is noticed at the 1st and 4th feedlines, which is identical to the E-field as illustrated in Fig. 8 (b). Besides, the 2nd and 3rd corner-regions of the Ag ground plane parallel to the respective directors of the radiator experience strong magnetic field. Therefore, the radiation pattern of the resultant electromagnetic wave (EM wave) becomes unidirectional.

Fig. 9 (a) shows 3D-far field directivity radiation pattern of the nanoantenna where maximum directivity of 8.23 dBi is obtained. Fig. 9 (b) illustrates E-plane as well as H-plane polar plots for co-polarization with directivity as outcome. At 8.4 THz, the 3 dB angular widths or half power beamwidths (HPBW) for co-polarized E-Plane (θ_E) and H-Plane (θ_H) of the nanoantenna are 98.3° and 88.8°, respectively. The 2D and 3D radiation patterns for gain of the nanoantenna at 8.4 THz are depicted in Fig. 10 (a) and Fig. 10 (b). It is apparent that along the elevation plane, nanoantenna is radiating the EM wave with a maximum gain of 8.56 dB. From 2D radiation pattern, gain is around azimuth within theta of 0° to 60°.

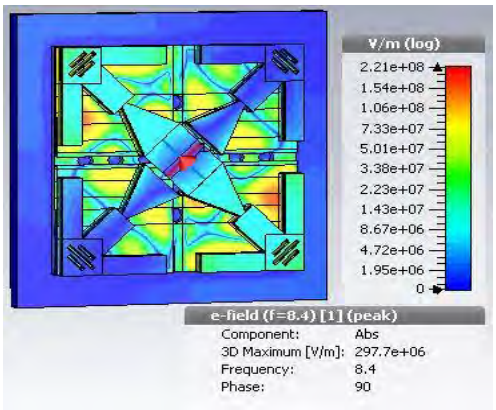

Fig. 8 (a). Plasmonic behavior of the proposed nanoantenna at 8.4 THz in terms of electric field

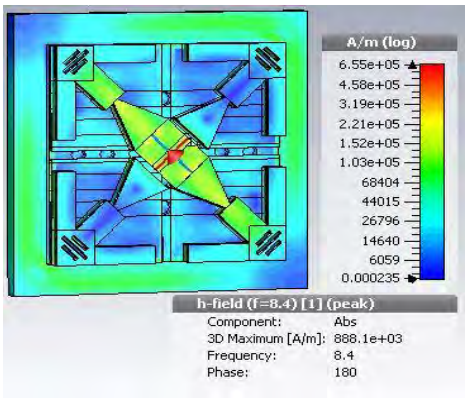

Fig. 8 (b). Plasmonic behavior of the proposed nanoantenna at 8.4 THz in terms of magnetic field

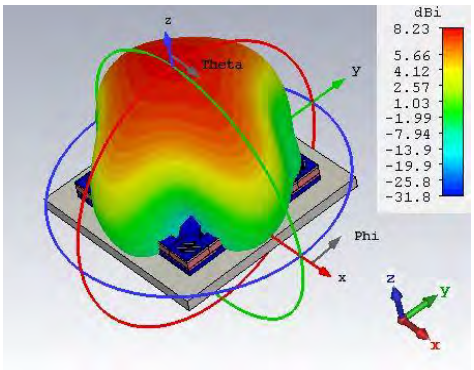

Fig. 9 (a). 3D plot of Far field directivity radiation pattern of the nanoantenna operating at 8.4 THz

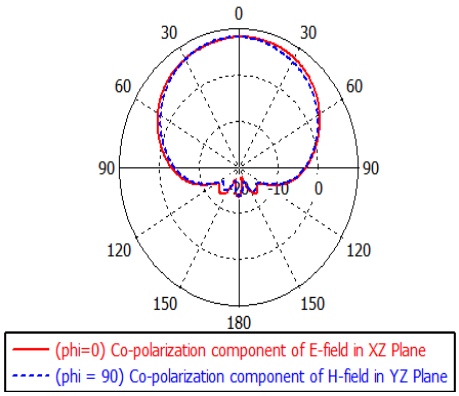

Fig. 9 (b). Co-polarization of electric and magnetic fields of the proposed nanoantenna operating at 8.4 THz

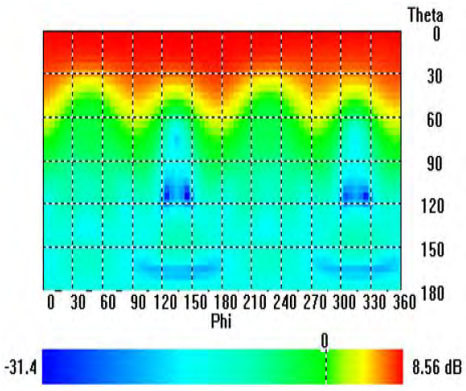

Fig. 10 (a). 2D radiation pattern for gain

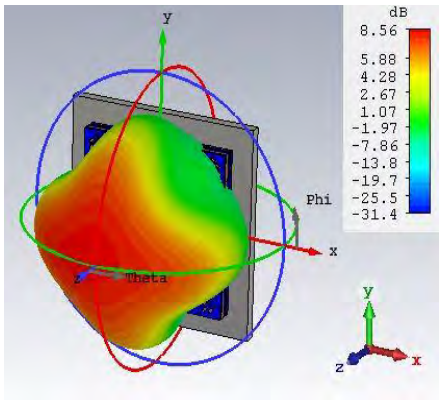

Fig. 10 (b). 3D radiation pattern for gain

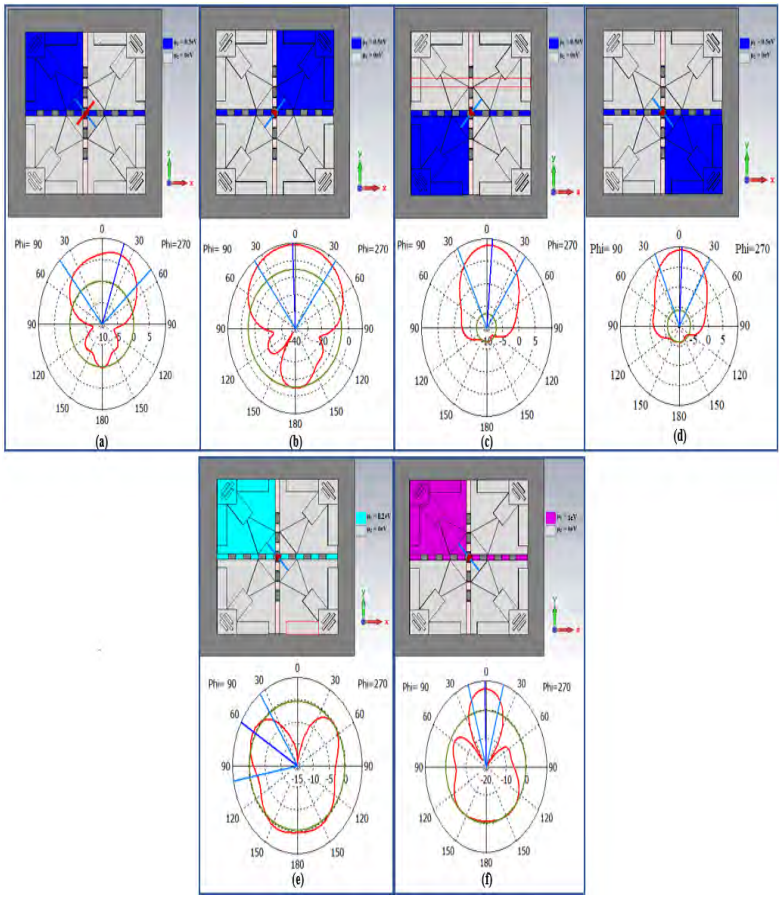

Fig. 11. Steered radiation pattern when applying gate potentials (0.2eV, 0.5eV, and 1eV) at the graphene patches and associated top graphene layer of the merged radiating structure

One of the important characteristics of our proposed GHPNA is its capability to steer the radiation beam dynamically from -2° to 60°, referring to Fig. 11 and Table III. Any one of the four intermediate graphene patches and associated top graphene layer of the merged radiating structure have been biased electrostatically such that they occupy μ_1 = 0.5 eV and remaining others have μ_2 = 0 eV as depicted in Fig. 11 (a-d). In Fig. 11 (a), once the main lobe direction has been changed to 20°, the directivity has decreased to 7.12 dBi. On the other hand, the directivities, e.g., 9.21 dBi, have been achieved although the steering angles have been less than 6° [Fig. 11 (b-d)]. Hence, an

inverse relationship between the main lobe direction and its magnitude has been observed. Indicating Fig. 11 (e, f), the chemical potential of upper-left graphene structure has been varied from 0.2 eV to 1 eV while maintaining others at 0 eV to get more steering angle. The graphene layers with minimum chemical potential (μ_1 = 0.2 eV) behave as closely as transparent media. As a result, a low directivity (0.523 dBi) and a large steering angle (60°) have been obtained from the composite radiating structure. The opposite radiation characteristics have been acquired for μ_1 = 1 eV as accumulated in Table III.

TABLE III. RADIATION CHARACTERISTICS OF THE PROPOSED GHPNA WHILE STEERING BEAM

Condition	Main Lobe Direction	Main Lobe Magnitude (dBi)	Angular Width (3dB)	Side Lobe Level (dB)
(a) Upper-Left Graphene Structure (0.5eV) & Others (0.0eV)	20°	7.12	58.2°	-8.7
(b) Upper-Right Graphene Structure (0.5eV) & Others (0.0eV)	-2°	8.85	74.9°	-14
(c) Bottom-Left Graphene Structure (0.5eV) & Others (0.0eV)	5°	8.55	62.6°	-15.3
(d) Bottom-Right Graphene Structure (0.5eV) & Others (0.0eV)	3°	9.21	55.5°	-15.1
(e) Upper-Left Graphene Structure (0.2eV) & Others (0.0eV)	60°	0.523	64.9°	-0.8
(f) Upper-Left Graphene Structure (1eV) & Others (0.0eV)	-1°	7.2	33.6°	-1.2

The notable features of the proposed GHPNA are compiled and comparison of our design with other graphene-based THz nanoantennas is carried out in Table IV. Our proposed graphene-based hybrid design has the capability of emitting the radiation pattern with the directivity and gain of 8.23 dBi and 8.56 dB, correspondingly, which are greater as compared to the nanoantennas resonating at the low THz wave spectrum [41 - 52]. The return loss of our proposed nano-scale THz antenna is -26.595 dB, which is lower than the graphene based triangular patch antenna [44] and the graphene microstrip patch ultrawide band antenna [50]. Besides, its BW is much wider in contrast to the reported graphene nanoantennas cited in literatures [43 - 45, 47, 49, 50]. Apart from these, our proposed GHPNA has an area of 12.96 μm^2, which is more compact than the reported THz nanoantennas.

TABLE IV. COMPARATIVE ANALYSIS AMONG PREVIOUSLY REPORTED THZ NANOANTENNAS WITH THE PROPOSED ONE

Ref.	Operating Frequency (f_r) (THz)	S_{11} (dB) at f_r	BW (GHz)	Gain (dB)	Directivity (dBi)
[43]	2.6	- 27	145.4	2.8	N[a]
[46]	6.43	- 48.75	N[a]	3.18	7.39
[48]	13	- 27.57	N[a]	5.30	5.32
[51]	0.81	-39	N[a]	N[a]	4.5
[52]	2.56-4.98	-33	2420	N[a]	5.56
[45]	5.491	- 48.88	231.3	4.06	5.455
[47]	7.32	- 50.78	371	6.34	7.899
[49]	6.994	- 75.66	386	7.29	7.408
[41]	0.750	- 35	N[a]	5.09	5.71
[42]	2.59	- 35.183	N[a]	5.03	7.19
[44]	2.7	- 13.66	90	6.59	6.91
[50]	1.75-2.25	-26	504	5.99	6.5
Proposed Antenna	8.4	-26.595	1241.3	8.56	8.23

[a.] Not Mentioned in the Research Work

V. CONCLUSION

A graphene-based hybrid plasmonic nanoantenna resonating in THz band has been designed and simulated using a commercially available finite element method (FEM) simulator known as "CST Microwave Studio". Providing suitable electrostatic gate bias voltage at every graphene patch and associated top graphene layer of the composite radiating structure has enabled the transverse magnetic SPP to resonate at THz frequencies. As a result, the radiation characteristics and beam direction have been altered from -2° to 60°. The perturbed silver layers, graphene sheets with cylindrical air defects, dielectric grating and metamaterial-based subwavelength slots have been modeled. As a consequence, gain, bandwidth and directivity of 8.56 dB, 1241.3 GHz, and 8.23 dBi, respectively, have been obtained. No side lobes, acceptable back lobes, and return loss of -26.595 dB have been acquired at the resonant frequency of 8.4 THz.

REFERENCES

[1] Koenig S, Lopez-Diaz D, Antes J, Boes F, Henneberger R, Leuther A, Tessmann A, Schmogrow R, Hillerkuss D, Palmer R, Zwick T, Koos C, Freude W, Ambacher O, Leuthold J, Kallfass I (2013) Wireless sub-THz communication system with high data rate. Nat Photonics 7:977-981

[2] R. Piesiewicz, T. Kleine-Ostmann, N. Krumbholz, D. Mittleman, M. Koch, J. Schoebei, and T. Kurner, "Short-range ultra-broadband terahertz communications: Concepts and perspectives," IEEE Antennas and Propagation Magazine, vol. 49, no. 6, pp. 24–39, 2007

[3] J. Federici and L. Moeller, "Review of terahertz and sub terahertz wireless communications," Journal of Applied Physics, vol. 107, no. 11, p. 111101, 2010

[4] H. Song and T. Nagatsuma, "Present and future of terahertz communications," IEEE Transactions on Terahertz Science and Technology, vol. 1, no. 1, pp. 256–263, Sep. 2011

[5] Akyildiz IF, Jornet JM, Han C (2014) Terahertz band: next frontier for wireless communications. Phys Commun 12:16-32

[6] T. S. Rappaport, Y. Xing, O. Kanhere, S. Ju, A. Madanayake, S. Mandal, A. Alkhateeb, and G. C. Trichopoulos, "Wireless communications and applications above 100 ghz: Opportunities and challenges for 6g and beyond," IEEE Access, vol. 7, pp. 78 729–78757, 2019

[7] Kaishun Wu, Jiang Xiao, Lionel M. Ni, Rethinking the architecture design of data center networks, Front. Comput. Sci. 6 (5) (2012) 596–603

[8] Poorgholam-Khanjari, S., & Zarrabi, F. B. (2021). Reconfigurable Vivaldi THz antenna based on graphene load as hyperbolic metamaterial for skin cancer spectroscopy. Optics Communications, 480. https://doi.org/10.1016/j.optcom.2020.126482

[9] Geetharamani, G., & Aathmanesan, T. (2020). Split ring resonator inspired THz antenna for breast cancer detection. Optics and Laser Technology, 126. https://doi.org/10.1016/j.optlastec.2020.106111

[10] Naftaly M, Foulds AP, Miles RE, Davies AG (2005) Terahertz transmission spectroscopy of nonpolar materials and relationship with composition and properties. Int J Infrared Millimet Waves 26(1):55-64

[11] Bin L et al (2018) Research progress on terahertz technology and its application in agriculture. Trans Chin Soc Agric Eng 34(2):1-9

[12] A. Davies, A. Burnett, W. Fan, E. Linfield, and J. Cunningham, "Terahertz spectroscopy of explosives and drugs", Materials Today, vol. 11, no. 3, pp. 18-26, 2008. Available: 10.1016/s1369-7021(08)70016-6

[13] Balamati Choudhury, Aniruddha R. Sonde, Rakesh Mohan Jha, Terahertz antenna technology for space applications, Terahertz Antenna Technology for Space

[14] T. Nagatsuma, G. Ducournau, and C. C. Renaud, "Advances in terahertz communications accelerated by photonics," Nature Photonics, vol. 10, no. 6, p. 371, 2016

[15] Q. Lu, D. Wu, S. Sengupta, S. Slivken, and M. Razeghi, "Room temperature continuous wave, monolithic tunable thz sources based on highly efficient mid-infrared quantum cascade lasers," Scientific reports, vol. 6, p. 23595, 2016

[16] "VDI passive devices," https://www.vadiodes.com/en/products/straight-waveguides-tapers-horn-antenna-directional-couplers, accessed: 2019-09-30

[17] "Mi-Wave Antennas," https://www.miwv.com/millimeter-wave-products/antenna-products/, accessed: 2019-09-30

[18] K. Fan, Z.-C. Hao, Q. Yuan, and W. Hong, "Development of a high gain 325–500 ghz antenna using quasi-planar reflectors," IEEE Transactions on Antennas and Propagation, vol. 65, no. 7, pp. 3384–3391, 2017

[19] N. Llombart, G. Chattopadhyay, A. Skalare, and I. Mehdi, "Novel terahertz antenna based on a silicon lens fed by a leaky wave enhanced waveguide," IEEE Transactions on Antennas and Propagation, vol. 59, no. 6, pp. 2160–2168, June 2011

[20] K. Konstantinidis, A. P. Feresidis, C. C. Constantinou, E. Hoare, M. Gashinova, M. J. Lancaster, and P. Gardner, "Low-thz dielectric lens antenna with integrated waveguide feed," IEEE Transactions on Terahertz Science and Technology, vol. 7, no. 5, pp. 572–581, Sep. 2017

[21] Han K et al (2010) Terahertz Yagi-Uda antenna for high input resistance. J. Infrared, Millim. Terahertz Waves 31.4:441-454

[22] Lin G, Huang F, Tang X (2014) A novel integrated MEMS helix antenna for terahertz applications. Optik-Inter J Light Electron Optic 125(1):101-103

[23] Kazemi, F. (2020). Dual band compact fractal THz antenna based on CRLH-TL and graphene loads. Optik, 206. https://doi.org/10.1016/j.ijleo.2020.164369

[24] Mak K-M, So K-K, Lai H-W, Luk K-M (2017) A magnetoelectric dipole leaky-wave antenna for millimeter wave application. IEEE Trans Antenn Propag 65(12):6395-6402

[25] HusseinA. Abdulnabi, Refat T. Hussein, Raad S. Fyath, 0.1-10Thz single port log periodic antenna design based on Hilbert graphene artificial magnetic conductor, (2006)

[26] Alharbi, Hamed K et al (2016) Diced and grounded broadband bow-tie antenna with tuning stub for resonant tunnelling diode terahertz oscillators, IET Microw. Antennas Propag 11.3:310-316

[27] Castro Neto AH, Guinea F, Peres NMR, Novoselov KS, Geim AK (2009) The electronic properties of graphene. RevMod Phys 81(1): 109-162

[28] A. C. Ferrari, F. Bonaccorso, V. Fal'Ko, K. S. Novoselov, S. Roche, P. Bøggild, S. Borini, F. H. Koppens, V. Palermo, N. Pugno et al., "Science and technology roadmap for graphene, related two-dimensional crystals, and hybrid systems," Nanoscale, vol. 7, no. 11, pp. 4598–4810, 2015

[29] P. A. D. Gonçalves and N. M. Peres, An introduction to graphene plasmonics. World Scientific, 2016

[30] Llatser I, Kremers C, Chigrin D, Jornet JM, LemmeMC, Cabellos-Aparicio A, Alarc'on E (2012) Radiation characteristics of tunable graphene in the terahertz band. Radioeng. J. 21(4)

[31] T.-T. Kim, H. Kim, M. Kenney, H. S. Park, H.-D. Kim, B. Min, and S. Zhang, "Amplitude modulation of anomalously refracted terahertz waves with gated-graphene metasurfaces," Advanced Optical Materials, vol. 6, no. 1, p. 1700507, 2018

[32] B. Sensale-Rodriguez, R. Yan, M. M. Kelly, T. Fang, K. Tahy, W. S. Hwang, D. Jena, L. Liu, and H. G. Xing, "Broadband graphene terahertz modulators enabled by intraband transitions," Nature communications, vol. 3, p. 780, 2012

[33] P. K. Singh, G. Aizin, N. Thawdar, M. Medley, and J. M. Jornet, "Graphene-based plasmonic phase modulator for terahertz-band communication," in Proc. of the 10th European Conference on Antennas and Propagation (EuCAP). IEEE, 2016, pp. 1–5

[34] B. Sensale-Rodriguez, T. Fang, R. Yan, M.M. Kelly, D. Jena, L. Liu, H.G. Xing, Unique prospects for graphene-based terahertz modulators, Appl. Phys. Lett. 99 (2011)113104

[35] M. Tamagnone, J. Gomez-Diaz, J. R. Mosig, and J. Perruisseau-Carrier, "Reconfigurable terahertz plasmonic antenna concept using a graphene stack," Applied Physics Letters, vol. 101, no. 21, p. 214102, 2012

[36] J. M. Jornet and I. F. Akyildiz, "Graphene-based plasmonic nano-antenna for terahertz band communication in nanonetworks," IEEE Journal on selected areas in communications, vol. 31, no. 12, pp. 685–694, 2013, U.S. Patent No. 9,643,841, May 9, 2017 (Priority Date: Dec.6, 2013)

[37] J. M. Jornet and I. F. Akyildiz, "Graphene-based plasmonic nano-transceiver for terahertz band communication," in Proc. of the 8th European Conference on Antennas and Propagation (EuCAP). IEEE, 2014, pp. 492–496, U.S. Patent No. 9,397,758, July 19, 2016 (Priority Date: Dec. 6, 2013)

[38] M. Nafari, G. R. Aizin, and J. M. Jornet, "Plasmonic hemt terahertz transmitter based on the dyakonov-shur instability: Performance analysis and impact of nonideal boundaries," Physical Review Applied, vol. 10, no. 6, p. 064025, 2018

[39] D. Schall, D. Neumaier, M. Mohsin, B. Chmielak, J. Bolten, C. Porschatis, A. Prinzen, C. Matheisen, W. Kuebart, B. Junginger, W. Templ, A.L. Giesecke, H. Kurz,50 GBit/s photodetectors based on wafer-scale Graphene for integrated silicon photonic communication systems, ACS Photonics 1 (2014) 781

[40] I.F. Akyildiz, J.M. Jornet, Electromagnetic wireless nanosensor networks, NanoCommun. Netw. 1 (2010) 3 –19

[41] Anand SS, Kumar DS, Wu RJ, Chavali M (2014) Graphene nanoribbon-based terahertz antenna on polyimide substrate, Optik. Science Direct 125:5546-5549

[42] Mrunalini S, Manoharan A (2017) Dual-band re-configurable graphene-based patch antenna in terahertz band for wireless network-on-chip applications. In: IET Microwaves, Antennas & Propagation, Volume 11, Issue 14, pp 2104-2108. https://doi.org/10.1049/iet-map.2017.0415

[43] George JN, Madhan MG (2017) Analysis of single band and dual band graphene-based patch antenna for terahertz region. Phys E Low Dimension Syst Nanostruct 94(October):126-131

[44] Bala R, Marwaha A (2015) "Development of computational model for tunable characteristics of graphene based triangular patch antenna in THz regime" Springer on Journal of Computational Electronics, ISSN- 1569-8025, indexed by SCI, Thomson Reuter journal list, Impact Factor 1.520, https://doi.org/10.1007/s10825-015-0761-6, Print ISSN 1569-8025, Online ISSN 1572-8137, pp 1.6, online 2015

[45] Khan MAK, Shaem TA, Alim MA (2019) Analysis of graphene based miniaturized terahertz patch antennas for single band and dual band operation. Optik 194:194. https://doi.org/10.1016/j.ijleo.2019.163012

[46] Thampy AS, DarakMS, Dhamodharan SK (Oct. 2015) Analysis of graphene-based optically transparent patch antenna for terahertz communications. Physica E: Low-dimensional Systems and Nanostructures 66:67-73

[47] Khan MAK, Shaem TA, Alim MA (2020) Graphene patch antennas with different substrate shapes and materials. Optik 202: 163700. https://doi.org/10.1016/j.ijleo.2019.163700

[48] Bala R, Marwaha A (2015) Characterization of graphene for performance enhancement of patch antenna in THz region. Optik - Int.J. Light Electron Opt. https://doi.org/10.1016/j.ijleo.2015.11.029

[49] Khan, M.A.K., Ullah, M.I., Kabir, R. et al. High-Performance Graphene Patch Antenna with Superstrate Cover for Terahertz Band Application. Plasmonics 15, 1719–1727 (2020). https://doi.org/10.1007/s11468-020-01200-z

[50] Dashti M, Carey JD. Graphene microstrip patch Ultrawide band antennas for THz communications. Adv Funct Mater. 2018;28(11):1705925

[51] Dash, S., Patnaik, A. Performance of Graphene Plasmonic Antenna in Comparison with Their Counterparts for Low-Terahertz Applications. Plasmonics 13, 2353–2360 (2018). https://doi.org/10.1007/s11468-018-0761-z

[52] Dash, S., Patnaik, A. and Kaushik, B., 2018. Performance enhancement of graphene plasmonic nanoantennas for THz communication. IET Microwaves, Antennas & Propagation, 13(1), pp.71-75

[53] M. Jablan, H. Buljan, and M. Soljačić, "Plasmonics in graphene at infrared frequencies," Phys. Rev. B -Condens. Matter Mater. Phys., vol. 80, no. 24, p. 245435, Dec. 2009.

[54] D. Correas-Serrano, J. S. Gomez-Diaz, J. Perruisseau-Carrier, and A. Alvarez-Melcon, "Spatially dispersive graphene single and parallel plate waveguides: Analysis and circuit model," IEEE Trans. Microw. Theory Tech., vol. 61, no. 12, pp. 4333–4344, Dec. 2013.

[55] D. Correas-Serrano, J. S. Gomez-Diaz, J. Perruisseau-Carrier, and A. Alvarez-Melcon, "Graphene-based plasmonic tunable low-pass filters in the terahertz band," IEEE Trans. Nanotechnol., vol. 13, no. 6, pp. 1145–1153, Nov. 2014.

[56] Vakil A, Engheta N (2011) Transformation optics using graphene. Science 332:1291–1294

[57] Nair RR, Blake P, Grigorenko AN, Novoselove KS, Booth TJ, Stauber T, Peres NMR, Geim AK (2008) Fine structure constant defines visual transparency of graphene. Science 320:1308

[58] Cubukcu E, Capasso F (2009) Optical nano rod antennas as dispersive one-dimensional Fabry–Pérot resonators for surface plasmons. Appl Phys Lett 95:201101

[59] GusyninV, Sharapov S, Carbotte J (2006) Magneto-optical conductivity in graphene. J Phys Condens Matter 19(1–28):026222

[60] Zeng, C., Liu, X., Wang, G.: 'Electrically tunable graphene plasmonic quasicrystal metasurfaces for transformation optics', Sci. Rep., 2014, 4, (5763), pp. 1–8

[61] Chen, P.Y., Alu, A.: 'Atomically thin surface cloak using graphene monolayers', ACS Nano, 2011, 5, pp. 5855–5863

[62] Jablan, M., Buljan, H., Soljacic, M.: 'Plasmonics in graphene at infrared frequencies', Phys. Rev. B, 2009, 80, p. 24535 (1–7)

[63] Hu, X. & Wang, J. High figure of merit graphene modulator based on long-range hybrid plasmonic slot waveguide. IEEE J. Quantum Electron. 53, 7200308 (2017).

[64] Lu, Z. & Zhao, W. Nanoscale electro-optic modulator based on graphene-slot waveguides. J. Opt. Soc. Am. B 29, 1490–1496 (2012)

[65] Liu, R. et al. Experimental demonstration of electro- magnetic tunneling through an epsilon-near-zero metamaterial at microwave frequencies. Phys. Rev. Lett. 100, 023903 (2008)

[66] Constantine A. Balanis, Antenna Theory Analysis and Design, New Jersey: John Wiley & Sons, Inc., Fourth Edition 2016

[67] Soliman, E. A., Sallam, M. O. & Vandenbosch, G. A. V. Plasmonic grid array of gold nanorods for point-to-point optical communications. IEEE J. Lightw. Technol. 32, 4296–4301 (2014).

[68] Khaleque, A. et al. Integration of bowtie plasmonic nano-antennas on tapered fiber. Opt. Express 25, 8986–8996 (2017).

[69] Pozar, D.M.: Considerations for millimeter wave printed antennas. IEEE Trans. Antennas Propag. 31(5), 740 –747 (1983)

[70] Grischkowsky, D., Duling III, I.N., Chen, T.C., Chi, C.-C.: Electromagnetic shock waves from transmission lines. Phys. Rev. Lett.59(15), 1663–1666 (1987)

[71] R. Garg, P. Bhartia, I. J. Bahl, and A. Ittipiboon, "Microstrip antenna design handbook", Artech house, 2001.

[72] Li, L., Chen, Q., Yuan, Q., Liang, C., & Sawaya, K. (2008). Surface-wave suppression band gap and plane-wave reflection phase band of mushroomlike photonic band gap structures. Journal of Applied Physics, 103(2). https://doi.org/10.1063/1.2832401

[73] Li J, He M, Wu C, Zhang C. Radiation-pattern-reconfigurable graphene leaky-wave antenna at terahertz band based on dielectric grating structure. IEEE Antennas Wireless Propagation Lett. 2017; 16:1771 -1775

[74] Schwering FK, Peng S-T. Design of dielectric grating antennas for millimeter-wave applications. IEEE Trans Microwave Theory Techniq. 1983;31(2):199-209

[75] Kushwaha RK, Karuppanan P. Parasitic-coupled high-gain graphene antenna employed on PBG dielectric grating substrate for THz applications. Microw Opt Technol Lett. 2020; 62:439–447. https://doi.org/10.1002/mop.32033

[76] Kushwaha, R. K., & Karuppanan, P. (2020). Enhanced radiation characteristics of graphene-based patch antenna array employing photonic crystals and dielectric grating for THz applications. Optik, 200. https://doi.org/10.1016/j.ijleo.2019.163422

[77] Martini, E., Mencagli, M. Jr. & Maci, S. Metasurface transformation for surface wave control. Philos. Trans. R. Soc. A 373, 20140355 (2015)

[78] Finch, M. F. & Lail, B. A. Multi-coupled resonant splitting with a nano-slot metasurface and PMMA phonons. In Proc. SPIE 9547, Plasmonics: Metallic Nanostructures and Teir Optical Properties XIII, 954710, 28, 1–6 (2015)

[79] Ignacio Llatser, Christian Kremers, Albert Cabellos-Aparicio, Josep Miquel Jornet, Eduard Alarcón, and Dmitry N. Chigrin, Graphene-based nano-patch antenna for terahertz radiation, Photonics and Nanostructures -Fundamentals and Applications 10 (2012), no. 4, 353_358

Richard Victor Biswas has received his B.Sc. and M.Sc. in Electrical and Electronic Engineering (EEE) from American International University Bangladesh (AIUB). He had been working as a teaching assistant in the department of EEE and Mechanical Engineering at Sonargaon University (SU) for two years. Currently, he is working as an Assistant Engineer (Analog Circuit Design) in the department of Silicon Engineering at Ulkasemi Pvt. Limited. His research interest incorporates analog and mixed-signal VLSI circuit designs, semiconductor device physics, terahertz wireless communications, photonic ICs, plasmonic devices etc.

Farhadur Arifin received his B.Sc. Degree in Electrical and Electronic Engineering from Bangladesh University of Engineering and Technology (BUET), Dhaka, Bangladesh in 2000, and M.Sc. Degree in Electrical Engineering from Royal Institute of Technology (KTH), Stockholm, Sweden in 2005. Currently he is working as an Associate Professor in the department of EEE and CoE at American International University- Bangladesh (AIUB). He is an active IEEE member & volunteer for last 8 years. He has 17 years of teaching experience and has extensive research experiences in universities of different EU countries such as Sweden, Finland, Germany, and Belgium. He has published more than thirty-five peer-reviewed papers in the domain of electrical and electronic engineering. His research interests include wireless communications, antennas and propagation, WBAN, VLSI circuit design, system on chip design and RF integrated circuit design.